View metadata, citation and similar papers at core.ac.uk

brought to you by CORE

provided by Nottingham ePrints

Novikov, S.V. and Foxon, C.T. (2017) Unintentional boron incorporation in AlGaN layers grown by plasma-assisted MBE using highly efficient nitrogen RF plasma-sources. Journal of Crystal Growth . ISSN 0022-0248

Access from the University of Nottingham repository:
http://eprints.nottingham.ac.uk/39910/8/CRYS23975_paper_060217.pdf

Copyright and reuse:

The Nottingham ePrints service makes this work by researchers of the University of Nottingham available open access under the following conditions.

This article is made available under the Creative Commons Attribution licence and may be reused according to the conditions of the licence. For more details see: http://creativecommons.org/licenses/by/2.5/

A note on versions:

The version presented here may differ from the published version or from the version of record. If you wish to cite this item you are advised to consult the publisher's version. Please see the repository url above for details on accessing the published version and note that access may require a subscription.

For more information, please contact eprints@nottingham.ac.uk

Journal of Crystal Growth (xxxx) xxxx–xxxx

Contents lists available at ScienceDirect

Journal of Crystal Growth

journal homepage: www.elsevier.com/locate/jcrysgro

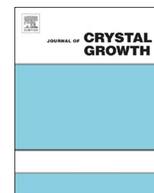

Unintentional boron incorporation in AlGaN layers grown by plasma-assisted MBE using highly efficient nitrogen RF plasma-sources

S.V. Novikov*, C.T. Foxon

School of Physics and Astronomy, University of Nottingham, Nottingham NG7 2RD, UK

ARTICLE INFO

Communicated by Dr Jean-Baptiste Rodriguez

Keywords:
A3. Molecular beam epitaxy
B1. Nitrides
A1. Doping
B2. Semiconducting III–V materials

ABSTRACT

Plasma-assisted molecular beam epitaxy (PA-MBE) is now widely used for the growth of group III-nitrides. Many years ago it became clear that during PA-MBE there is unintentional doping of GaN with boron (B) due to decomposition of the pyrolytic boron nitride (PBN) cavity of the RF plasma source. In this paper we discuss the unintentional B incorporation for PA-MBE growth of GaN and $Al_xGa_{1-x}N$ using a highly efficient RF plasma source. We have studied a wide range of MBE growth conditions for GaN and $Al_xGa_{1-x}N$ with growth rates from 0.2 to 3 µm/h, RF powers from 200 to 500 W, different nitrogen flow rates from 1 to 25 sccm and growth times up to several days. The chemical concentrations of B and matrix elements of Al, Ga, N were studied as a functions of depth using secondary ion mass spectrometry (SIMS). We demonstrate that boron incorporation with this highly efficient RF plasma source is approximately 1×10^{18} to 3×10^{18} cm^{-3} for the $Al_xGa_{1-x}N$ growth rates of 2 – 3 µm/h.

1. Introduction

Plasma-assisted molecular beam epitaxy (PA-MBE) is now widely used for the growth of group III-nitride layers and device structures.

Many years ago it became clear that in PA-MBE using a nitrogen RF plasma source there is unintentional doping of the layers with boron (B) due to decomposition of pyrolytic boron nitride (PBN) cavity and the PBN aperture plate of the RF plasma source [1]. It was established that the boron background concentration in unintentionally doped GaN depended strongly on the RF power for the plasma nitrogen source [2].

Molecular beam epitaxy is normally regarded as an epitaxial technique for the growth of very thin layers with monolayer control of their thickness. However, we have recently used the PA-MBE technique for bulk crystal growth and have produced free-standing layers of zinc-blende and wurtzite GaN and $Al_xGa_{1-x}N$ up to 100 µm in thickness [3,4]. In our initials studies we have used an HD25 nitrogen plasma source from Oxford Applied Research and the growth rate for $Al_xGa_{1-x}N$ films remained below 0.6 µm/h which is too slow to make the process commercially viable.

Recent years there have seen significant efforts from the main MBE manufacturers in France, USA and Japan to increase the efficiency of their nitrogen RF plasma sources to allow higher growth rates for GaN-based alloys [5–8]. Majority of the manufacturers are exploring the route of increasing the conductance of the aperture plates of the RF plasma cavity in order to achieve significantly higher total flows of nitrogen through the plasma source. In the recent Riber source the conductance of the aperture plate has been increased by increasing the number of 0.3 mm diameter holes initially to 1200 [5] and later to 5880 holes in the aperture plate [6]. First tests of the latest model of Riber RF nitrogen plasma source with 5880 holes in the aperture plate, produced even higher growth rates for thin GaN layers up to 7.6 µm/h, but with nitrogen flow rates of about 25 sccm [6]. Veeco is following the same path, in their latest design they have replaced original plasma aperture with a 5.6 times higher conductance aperture in order to allow for higher gas flow while maintaining the high-brightness RF nitrogen plasma mode [7]. First tests of the new Veeco's source demonstrated growth rates for thin GaN layers up to 9.8 µm/h, which was achieved using 20 sccm of N_2 and 7.7 sccm Ar flows at 600 W of RF power [7].

During the last few years, we have compared different RF nitrogen plasma sources for the growth of thick free-standing wurtzite $Al_xGa_{1-x}N$ films [9,10]. The novel high efficiency RF plasma source allowed us to achieve such free-standing $Al_xGa_{1-x}N$ samples on 3-in. diameter substrates in a single day's growth, which makes our bulk growth technique potentially commercially viable. We are using a highly efficient RF plasma source with high nitrogen flows and high RF powers. Our GaN growth rates reached 3 µm/h, which is about one order of magnitude higher than in our earlier studies. Therefore, one can expect that the PBN cavity decomposition and unintentional B incorporation could become significantly more intense.

* Corresponding author.
E-mail address: Sergei.Novikov@Nottingham.ac.uk (S.V. Novikov).

http://dx.doi.org/10.1016/j.jcrysgro.2017.01.007

0022-0248/ © 2017 The Authors. Published by Elsevier B.V.
This is an open access article under the CC BY license (http://creativecommons.org/licenses/BY/4.0/).

In this study we have investigated the influence of the PA-MBE conditions on unintentional boron (B) incorporation in GaN and $Al_xGa_{1-x}N$ layers grown with the wide range of RF plasma sources.

2. Experimental details

Wurtzite GaN and $Al_xGa_{1-x}N$ films were grown by PA-MBE in a MOD-GENII system [9,10]. 2-in. and 3-in. diameter sapphire and GaAs (111)B were used as substrates. The active nitrogen for the growth of the group III-nitrides was provided by HD25 nitrogen plasma source from Oxford Applied Research and a novel high efficiency plasma source from Riber RF-N 50/63 with 5880 holes in the aperture plate. The source was custom designed at Riber in order to match the dimensions of MOD-GENII Varian system. The use of an As_2 flux of ~6×10^{-6} Torr beam equivalent pressure (BEP) during substrate heating and the removal of the surface oxide from the GaAs (111)B substrates allowed us to avoid any degradation of the GaAs substrate surface prior to growth. The arsenic flux was terminated at the start of the GaN growth. A thin GaN buffer was deposited before the growth of the $Al_xGa_{1-x}N$ layers. In the current study, the $Al_xGa_{1-x}N$ layers were grown at temperatures of ~700 °C. We are not able to use higher growth temperatures due to the low thermal stability of the GaAs substrates in vacuum above 700 °C, even under an As_2 flux.

$Al_xGa_{1-x}N$ layers with thicknesses up to 100 µm were grown on GaAs substrates and the GaAs was subsequently removed using a chemical etch to achieve free-standing $Al_xGa_{1-x}N$ wafers. From our previous experience with MBE growth of bulk zinc-blende and wurtzite $Al_xGa_{1-x}N$ [3,4], such thicknesses are already sufficient to obtain free-standing $Al_xGa_{1-x}N$ layers.

The structural properties of the samples were studied *in-situ* using reflection high-energy electron diffraction (RHEED) and after growth *ex-situ* measurements were performed using X-ray diffraction (XRD) and transmission electron microscopy (TEM).

The chemical concentrations of B and matrix elements of Al, Ga, N were studied as a function of depth using secondary ion mass spectrometry (SIMS) in two commercial systems a Cameca IMS-3F and a Cameca IMS-4F system. The analysis of the samples was carried out using O_2^+ primary ion bombardment and positive secondary ion detection to optimize sensitivity to boron. The data were quantified using reference samples of boron implanted into commercial bulk GaN, AlN and GaAs wafers. We have used commercial bulk GaN wafers from Ammono and bulk AlN wafers from HexaTech.

3. Results and discussion

Fig. 1 shows SIMS depth profiles for B, Ga, Al and As for a $Al_xGa_{1-x}N$ layer (x~0.2) grown on GaAs (100) substrate with the HD-25 plasma source. For growth of the $Al_xGa_{1-x}N$ layer we have used group III-rich conditions, a N_2 flow of 1 sccm, an RF power 450 W and a growth time 2 h. We have achieved a growth rate of ~0.25 µm/h. The boron concentration was quantified using reference samples of boron implanted standards and is presented on the left axis. To study Ga we have used $^{69}G^{14}N$ ions signal, to study Al we have use $^{27}Al^{14}N$ ions signal and ^{75}As ions for arsenic. The signals for Ga, Al and As were not quantified and are presented in arbitrary units on the right axis. We can clearly observe the position of the AlGaN/GaAs interface by the drop of B and N-containing signals and the increase of the As signal and have ploted vertical dash line in Fig. 1 to mark the approximate position the AlGaN/GaN interface. We observed a gradual decrease of the SIMS signals for B and N-containing ions in the GaAs layer. This is not due to diffusion of Al, Ga or B into GaAs, but is a SIMS artifact due to roughening of the crater during sputtering. The boron concentration in the $Al_xGa_{1-x}N$ layer is relatively constant and is ~7–8×10^{17} cm^{-3}. We have studied several $Al_xGa_{1-x}N$ layers grown under similar MBE growth conditions with the HD-25 plasma source and we have observed boron incorporation levels similar to Fig. 1.

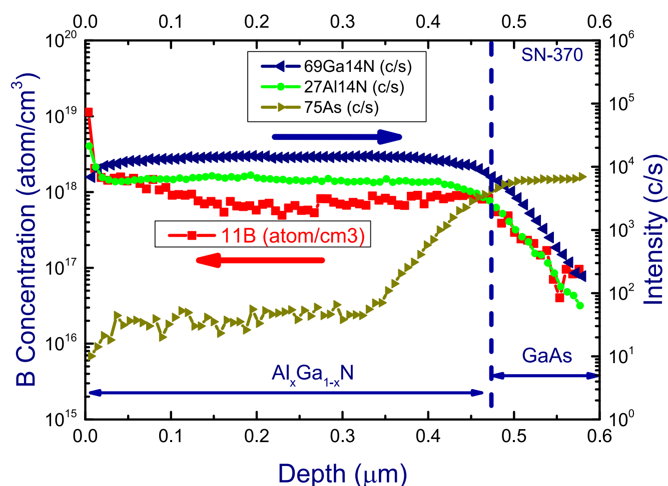

Fig. 1. SIMS profiles for B, Ga, Al and As for a $Al_xGa_{1-x}N$ layer (x~0.2) grown with an HD-25 plasma source (1 sccm N_2 flow rate, 450 W, t=2 h and growth rate ~0.25 µm/h).

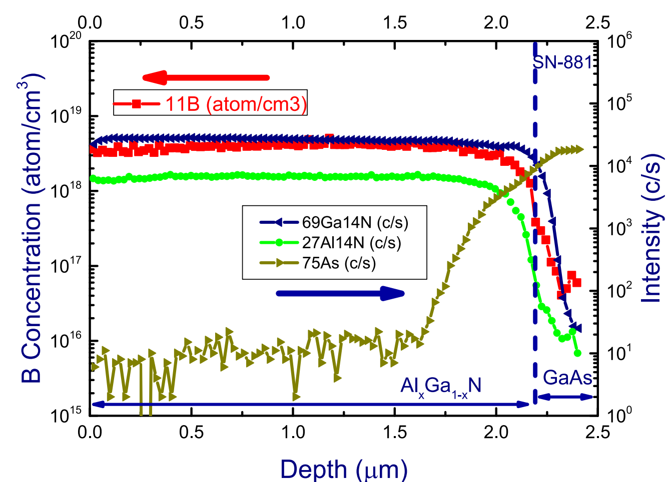

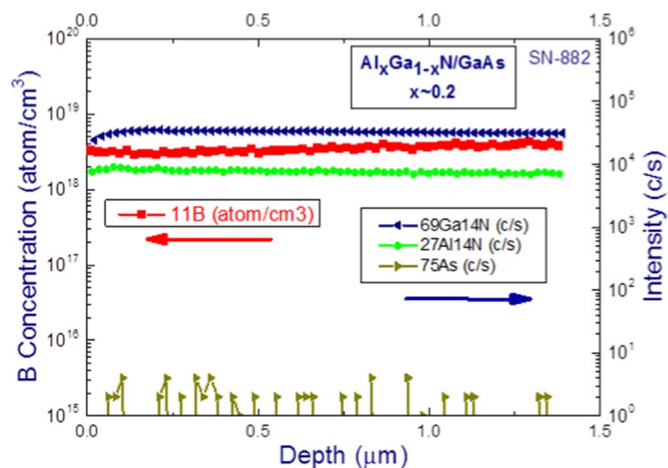

Fig. 2. SIMS profiles for B, Ga, Al and As for a w-$Al_xGa_{1-x}N$ layer (x~0.2) grown with a Riber plasma source a) t=1 h; b) t=43 h (6 sccm N_2 flow rate, 500 W and growth rate ~2.25 µm/h).

Fig. 2 shows SIMS profiles for B, Ga, Al and As for a w-$Al_xGa_{1-x}N$ layer (x~0.2) grown with the highly efficient Riber RF plasma source. We have grown the $Al_xGa_{1-x}N$ layer under group III-rich conditions, with a N_2 flow of 6 sccm and an RF power of 500 W. Fig. 2a presents SIMS data for the $Al_xGa_{1-x}N$ layer grown on a 2″ GaAs (111)B substrate for 1 h. The position of the $Al_xGa_{1-x}N$/GaAs interface is

clearly indicated by the decrease of all N-containing signals and an increase of As signal. With the new Riber source we have achieved a growth rate ~2.25 µm/h, which is about one order faster than in the case of HD-25 source results presented in Fig. 1. The boron concentration in $Al_xGa_{1-x}N$ layer in Fig. 2a is uniform through the layer and is ~3×10^{18} cm^{-3}.

High-resolution TEM studies were used to investigate the interface between the GaAs substrate and GaN layer and results are already published elsewhere [11]. We observed zinc-blende AlGaN crystallites in the wurtzite AlGaN matrix close to the GaAs substrate interface. These cubic inclusions extend to the first few tens of nanometers into the $Al_xGa_{1-x}N$ wurtzite film, before being terminated at (0001) basal plane stacking faults, which form boundaries with the wurtzite matrix. We also see the roughening of the surface of the GaAs due to nitrogen RF plasma-etching or Ga-Al melt-back etching of the GaAs substrate. Arsenic contamination of the first few hundreds nanometers of the layer is responsible for the formation of the zinc-blende grains. This initial As contamination at the start of the $Al_xGa_{1-x}N$ growth can be clearly observed by SIMS in Fig. 1 and Fig. 2a.

Fig. 2b presents SIMS data for a thick (~95 µm) $Al_xGa_{1-x}N$ layer, grown on 2″ GaAs (111)B for 43 h under the conditions similar to the sample presented on Fig. 2a, so with a growth rate ~2.25 µm/h. Using SIMS, it is not cost effective to try to sputter through the entire 100 µm of the layer to see the $Al_xGa_{1-x}N$/GaAs interface. Therefore, Fig. 2b presents SIMS data from the top ~1.5 µm of $Al_xGa_{1-x}N$ layer. The arsenic concentration is below or just on the level of sensitivity of SIMS system. The boron concentration in $Al_xGa_{1-x}N$ layer in Fig. 2b is also uniform through the layer and is at the same level of ~3×10^{18} cm^{-3}. It is very important to highlight that the boron concentration in the $Al_xGa_{1-x}N$ layers presented in Figs. 2a and b is practically identical and has not changed after 2 days of continuous MBE growth using the Riber RF plasma source. We have studied several $Al_xGa_{1-x}N$ layers grown under similar MBE growth conditions with the Riber plasma source on 2″ and 3″ GaAs substrates and we have observed similar levels of boron incorporation to that shown in Fig. 2.

All $Al_xGa_{1-x}N$ layers in Figs. 1 and 2 were grown under group III-rich conditions, as established by our calibration growths. However, the fluxes to achieve that metal-rich conditions will be significantly different for two types of the RF-plasma sources. The Ga and Al beam equivalent pressures (BEP) for the growth of $Al_xGa_{1-x}N$ layer shown in Fig. 1 were 2.68 10^{-7} Torr and 3.73 10^{-8} Torr and for $Al_xGa_{1-x}N$ shown in Fig. 2a were 1.45 10^{-6} Torr and 2.02 10^{-7} Torr, respectively. With the higher growth rate and higher Ga and Al fluxes the growth window where we have group III rich conditions, but before the formation of metal droplets is narrower. Therefore, we can't guarantee that the metal droplets coverage on the samples presented in Figs. 1 and 2 are the same and the III:V ratio during the growth of these two samples may also be different. Metal droplets on the surface may influence boron incorporation. Therefore, we need to consider this when we comparing boron incorporation in the above two $Al_xGa_{1-x}N$ layer grown with the different RF plasma sources.

The growth rate for $Al_xGa_{1-x}N$ layers achieved with the Riber source is ~2.25 µm/h, which is about 10 times faster than that for the layers grown with the HD-25 source of ~0.25 µm/h. However, the boron concentration is only 4 times higher and increased from ~7–8×10^{17} cm^{-3} (Fig. 1) to ~3×10^{18} cm^{-3} (Fig. 2). Therefore, boron doping concentration in the layer is increasing for the GaN layers grown with the highly efficient source, but not as fast as the increase in growth rate. To understand this let's consider the growth parameters, which will influence the boron incorporation. The boron concentration in the layer will be equal to the total number of boron atoms in the GaN layer divided by the total volume of the GaN layer. The total boron amount in the layer is equal to the incoming boron flux (F) multiplied by the growth time (t) and growth area (S). The volume of GaN layer is equal to the growth rate (V) multiplied by growth time (t) and growth area (S), (see the equation 1). Therefore, boron concentration is

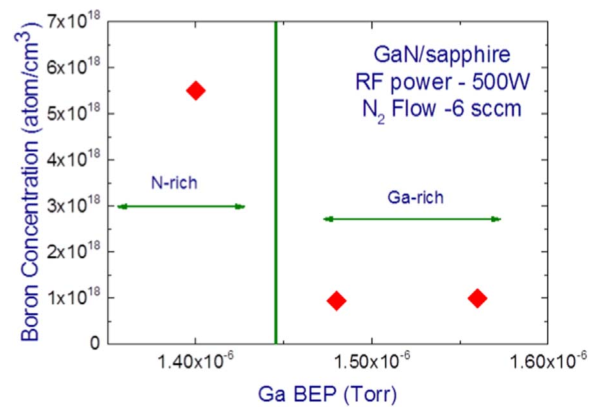

Fig. 3. SIMS boron concentration in GaN layers grown under N-rich and Ga-rich conditions with a Riber plasma source (6 sccm N_2 flow, 500 W and t=0.5 h).

proportional to the boron flux divided by the growth rate. This means that if, for example, the growth rate increases by a factor 10 and the boron flux also increases by a factor 10, the resulting boron concentration in the GaN will not change at all. Therefore, we can estimate from the levels in Figs. 1 and 2 that we have strong increase in the boron flux coming from the highly efficient RF plasma source. However, this resulted in a relatively small increase in the boron concentration because the growth rate is also higher. Therefore, the level of unintentional boron doping in GaN layers grown with a highly efficient plasma sources is only a few times higher than the boron concentration in layers grown with a standard RF plasma sources.

$$C_B = \frac{Total\ Boron}{Volume} = \frac{F\times t\times S}{V\times t\times S} = \frac{Flux\left(\frac{atom}{m^2 s}\right)}{Growth\ rate\left(\frac{\mu m}{h}\right)}$$

We have also found that boron incorporation is significantly different under N-rich and group III-rich growth conditions. Fig. 3 presents the SIMS boron concentration for GaN layers grown on sapphire using the Riber plasma source with a N_2 flow rate of 6 sccm, an RF power of 500 W and a growth time of 0.5 h. We have varied the Ga flux to be able to achieve GaN layers under N-rich and Ga-rich conditions. We can clearly see the transition in RHEED during the growth – spotty RHEED for N-rich and streaky for Ga-rich conditions. Therefore, we are able to put the vertical line in Fig. 3 to demonstrate the approximate position of the N-rich to Ga-rich boundary. The GaN growth rate has slightly increased with increasing Ga flux from 2.25 µm/h for the sample grown under N-rich conditions to 2.36 µm/h and 2.40 µm/h for two Ga-rich samples respectively. The boron incorporation is about 5 times stronger under N-rich growth conditions. GaN layers grown under N-rich conditions normally have a columnar structure. Therefore, boron can accumulate on the surface of the columns and not into the volume of the grains. That can explain very abrupt increase for B incorporation to the GaN layers grown under N-rich conditions.

Fig. 4 shows the dependence of the boron incorporation on the N_2 flow rate for the GaN layers grown on sapphire using the Riber plasma source with a fixed RF power of 500 W and growth time of 0.5 h. We have used a very broad range of the N_2 flows up to 25 sccm. All the GaN layers were grown under Ga-rich conditions. In order to sustain Ga-rich conditions the Ga flux was increased to keep the Ga to N_2 ratio constant. The boron incorporation decreases almost linearly with increasing N_2 flow rate. Because we have a fixed RF power this suggests that with increasing N_2 flow rate we are just diluting the concentration of boron atoms in the incoming nitrogen flux.

The boron incorporation depends strongly depends RF power we are using during the growth, as shown in Fig. 5a. The GaN layers were grown on sapphire with a fixed Ga beam equivalent pressure (BEP), a fixed N_2 flow of 6 sccm and a fixed growth time of 0.5 h. The boron incorporation

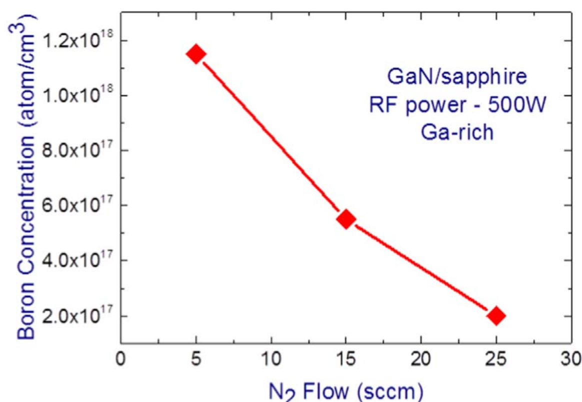

Fig. 4. SIMS boron concentration in GaN layers grown with a different N_2 flow rates under Ga-rich conditions with a Riber plasma source (500 W, t=0.5 h).

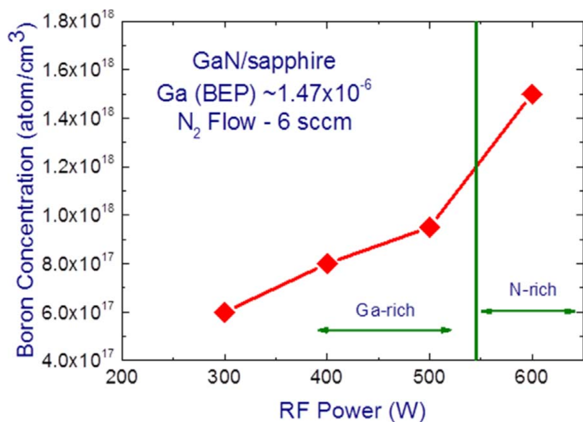

Fig. 5. a) SIMS boron concentration and b) growth rate for GaN layers grown with a different RF power with a Riber plasma source (6 sccm N_2 flow and t=0.5 h).

increases linearly with increasing RF power. However, for RF powers above 500 W, the rate of increase with power is enhanced. At that point we also observed a change in the RHEED pattern for growth of the GaN layer from streaky to spotty at an RF power of 600 W, which suggests that the growth has changed from Ga-rich to the N-rich conditions. The boron incorporation increases dramatically under N-rich condition as shown in Fig. 3, which is consistent with the change in the slope in Fig. 5a. However, the most important result from Fig. 5a is that the boron incorporation is proportional to RF power, which is consistent with earlier studies by other groups [2].

Fig. 5b presents the growth rate for the same set of GaN sample shown in Fig. 5a. For the Ga-rich conditions for RF powers between 300 W and 500 W we observed a linear increase of the GaN growth rate with RF power. The growth rate saturates for the RF powers higher than 500 W, which corresponds to N-rich conditions, where growth rate is limited by the fixed supply of group III element, in this case Ga.

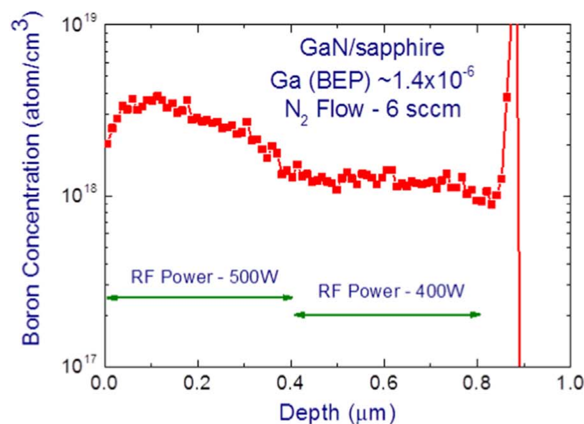

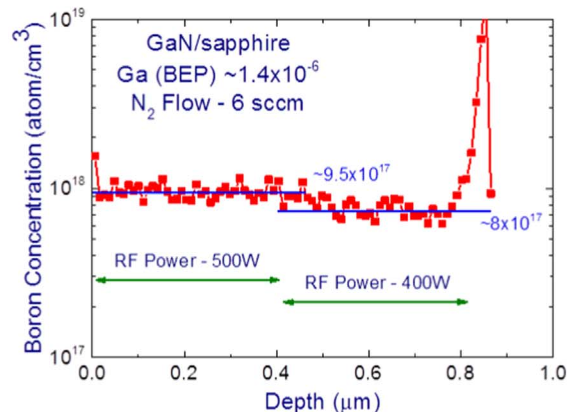

Fig. 6. SIMS profiles for B for a GaN layer grown with a step change in the RF power from 400 W to 500 W with a Riber plasma source a) at the centre of 2″ wafer; b) at the edge of 2″ wafer.

Fig. 6 demonstrates what happens to the boron incorporation if we change the RF power during the growth of the GaN layer. We have changed RF power from 400 W to 500 W in the middle of the growth process. At the beginning of the growth at an RF power of 400 W the RHEED for GaN growth was streaky and so we were growing under the Ga-rich conditions. At the end of the growth we observed a spotty RHEED pattern in the centre of 2-in. wafer and a streaky RHEED pattern at the edges of the wafer. Therefore, we can conclude that the growth mode was Ga-rich at the edges of the wafer, but was changed from Ga-rich at 400 W to N-rich at 500 W at the centre of the wafer. Fig. 6 shows a dramatic difference in the change of boron incorporation in the center of the wafer (Fig. 6a) and a small difference at the edges of the wafers (Fig. 6b). At the edge, Fig. 6b, we can see only a small increase in the boron incorporation, which is consistent with the data from Fig. 5 for the growth at 400 W and 500 W. However, at the centre of the wafer we see a dramatic increase in the boron incorporation in the middle of the growth, where we have changed to N-rich growth conditions as shown in Fig. 6a.

4. Summary and conclusions

We have discussed the unintentional B incorporation during PA-MBE growth of $Al_xGa_{1-x}N$ using a highly efficient RF plasma source. We have studied a wide range of MBE growth conditions with $Al_xGa_{1-x}N$ growth rates from 0.2 to 3 μm/h, RF powers from 200 W to 500 W, different nitrogen flow rates from 1 sccm to 25 sccm and for growth times up to several days. We have demonstrated that B incorporation with this highly efficient RF plasma sources is ~1×10^{18} to 3×10^{18} cm^{-3} for the $Al_xGa_{1-x}N$ growth rates 2–3 μm/h.

Acknowledgements

This work was supported by the Engineering and Physical Sciences Research Council (Grant no. EP/K008323/1). We want to acknowledge Loughborough Surface Analysis Ltd for SIMS measurements and discussions of results.

References

[1] R.M. Moldovan, L.S. Hirsch, A.J. Ptak, C.D. Stinespring, T.H. Myers, N.C. Giles, J. Electron. Mater. 27 (1998) 756.
[2] H. Kim, F.J. Falth, T.G. Andersson, J. Electron. Mater. 30 (2001) 1343.
[3] S.V. Novikov, N.M. Stanton, R.P. Campion, R.D. Morris, H.L. Geen, C.T. Foxon, A.J. Kent, Semicond. Sci. Technol. 23 (2008) 015018.
[4] S.V. Novikov, C.R. Staddon, R.E.L. Powell, A.V. Akimov, F. Luckert, P.R. Edwards, R.W. Martin, A.J. Kent, C.T. Foxon, J. Cryst. Growth 322 (2011) 23.
[5] B.M. McSkimming, F. Wua, T. Huault, C. Chaix, J.S. Speck, J. Cryst. Growth 386 (2014) 168.
[6] B.M. McSkimming, C. Chaix, J.S. Speck, J. Vac. Sci. Technol. A 33 (2015) 05E128.
[7] B.P. Gunning, E.A. Clinton, J.J. Merola, W.A. Doolittle, R.C. Bresnahan, J. Appl. Phys. 118 (2015) 155302.
[8] Y. Cordier, B. Damilano, P. Aing, C. Chaix, F. Linez, F. Tuomisto, P. Vennegues, E. Frayssinet, D. Lefebvre, M. Portail, M. Nemoz, J. Cryst. Growth 433 (2016) 165.
[9] S.V. Novikov, C.R. Staddon, S.-L. Sahonta, R.A. Oliver, C.J. Humphreys, C.T. Foxon, Phys. Status Solidi C. 13 (2016) 217.
[10] S.V. Novikov, C.R. Staddon, J. Whale, A.J. Kent, C.T. Foxon, J. Vac. Sci. Technol. B 34 (2016) 02L102.
[11] S.V. Novikov, C.R. Staddon, S.-L. Sahonta, R.A. Oliver, C.J. Humphreys, C.T. Foxon, J. Cryst. Growth 456 (2016) 151.